Supplementary materials

# The influence of electrolyte type on kinetics of redox processes in the polymer films of Ni(II) *salen* type complexes

D. Tomczyk*[1], P. Seliger[1], W. Bukowski[2], K. Bester[2]

## Figures

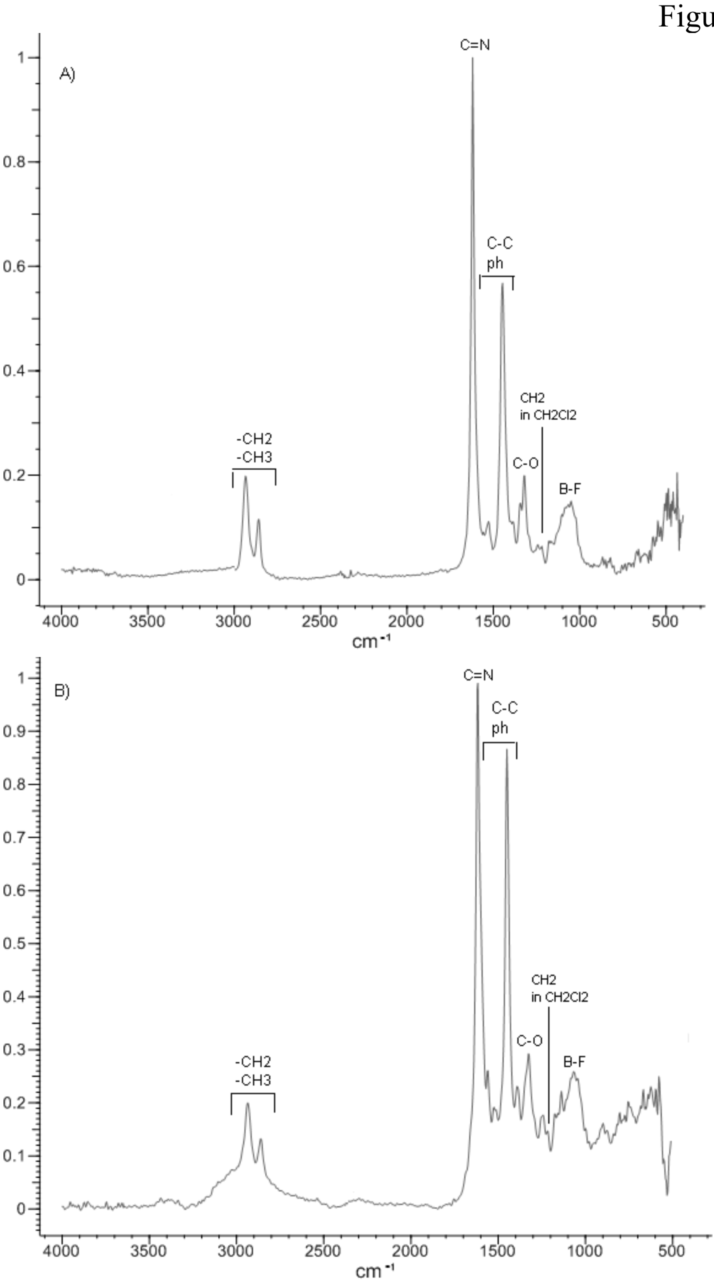


**Figure S1**. FTIR ATR spectra of *poly*[Ni(salcn(Me))] electrosynthesized in $TBABF_4/CH_2Cl_2$ (v = 0.05 $V \cdot s^{-1}$, 10 scans, vs. Ag/AgCl), A) - neutral, B) - oxidized at the anode peak potential, $E_{pa}$ = 0.6 V.

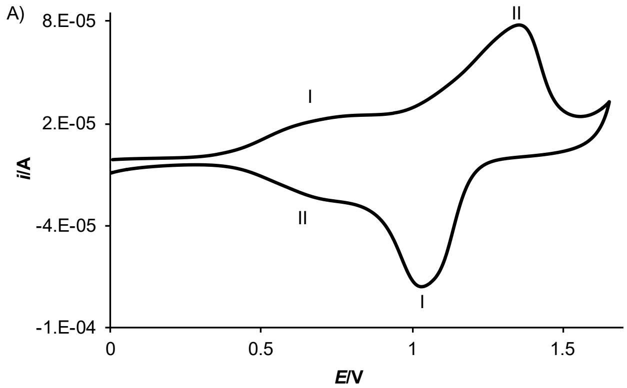


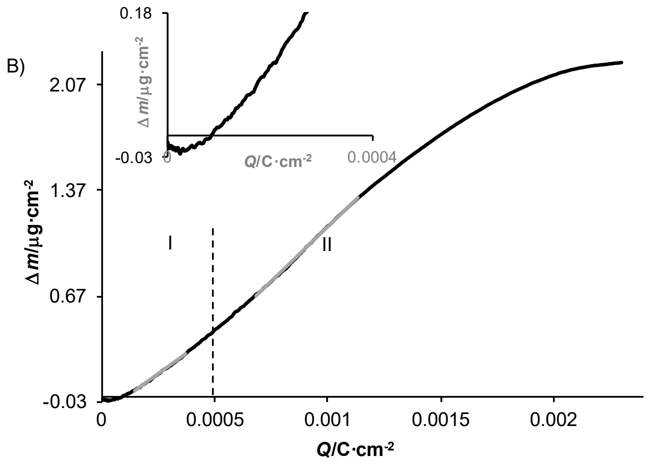


**Figure S2**. *Poly*[Ni(salcn)] (1 electropolymerization cycle) in $TBAPF_6/CH_2Cl_2$, Pt/quarzglas , $v = 0.05$ V·s$^{-1}$, vs. Ag/AgCl; A) cyclic voltammogram; B) plots $\Delta m$ vs $Q$ for anodic process; grey parts of the curve - trend lines for the $\Delta m = f(Q)$ relationship.

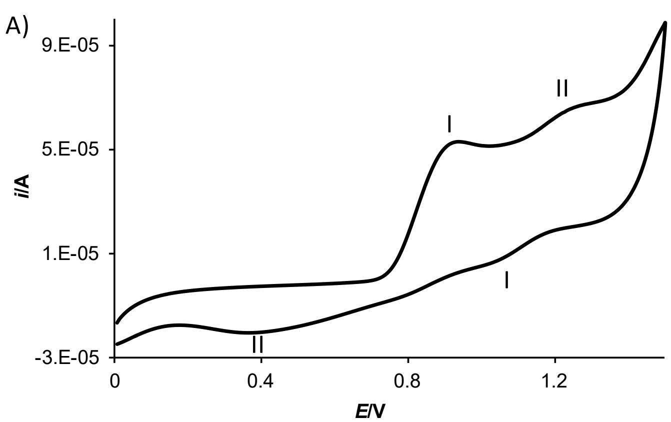

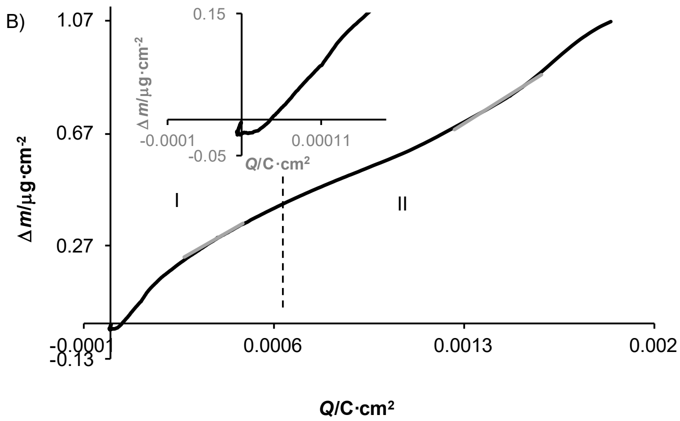


**Figure S3**. *Poly*[Ni(salcn)] (1 electropolymerization cycle) in $TBABF_4/CH_2Cl_2$, Pt/quarzglas , $v = 0.05$ V·s$^{-1}$, vs. Ag/AgCl; A) cyclic voltammogram; B) plots Δ*m* vs *Q* for anodic process; grey parts of the curve - trend lines for the Δ*m* = f(*Q)* relationship.

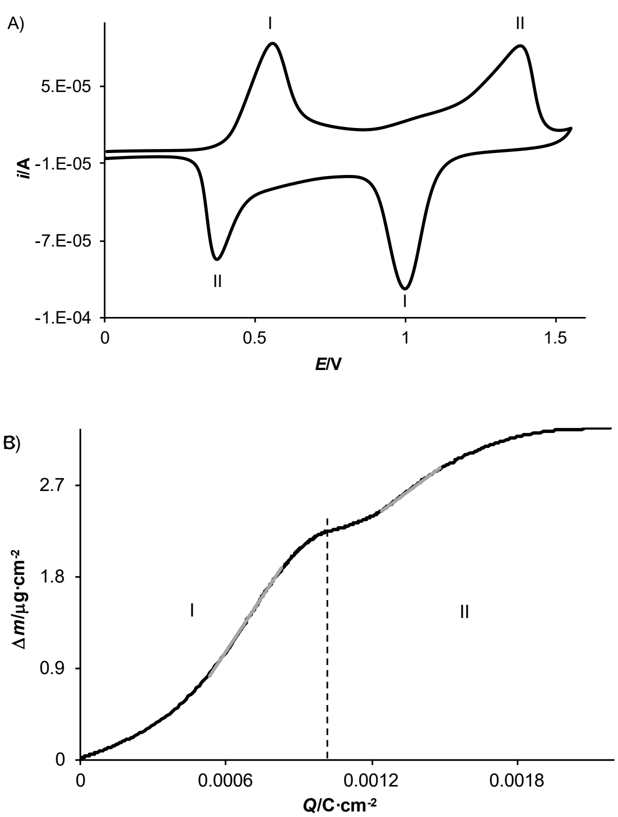


**Figure S4**. *Poly*[Ni(salcn(Me))] (1 electropolymerization cycle) in $TBAPF_6/CH_2Cl_2$, Pt/quarzglas , $v = 0.05$ V·s$^{-1}$, vs. Ag/AgCl; A) cyclic voltammogram; B) plot Δ*m* vs *Q* for oxidation process; grey parts of the curve - trend lines for the Δ*m* = f(*Q)* relationship.

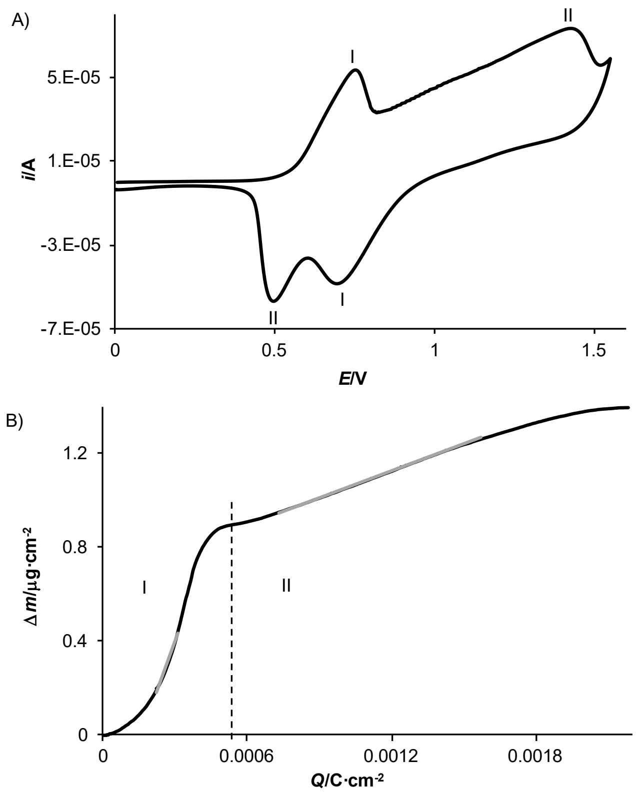


**Figure S5**. *Poly*[Ni(salcn(Me))] (1 electropolymerization cycle) in $TBABF_4/CH_2Cl_2$, Pt/quarzglas , $v = 0.05$ V·s$^{-1}$, vs. Ag/AgCl; A) cyclic voltammogram; B) plot Δ*m* vs *Q* for anodic process; grey parts of the curve - trend lines for the Δ*m* = f(*Q)* relationship.

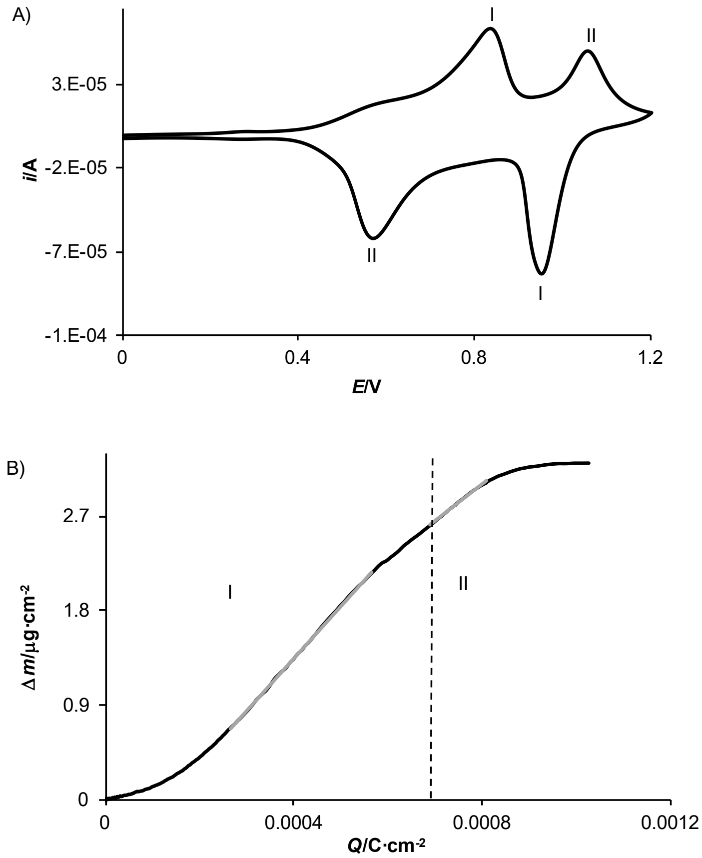


**Figure S6**. *Poly*[Ni(salcn(Bu))] (1 electropolymerization cycle) in $TBAPF_6/CH_2Cl_2$, Pt/quarzglas , $v = 0.05$ V·s$^{-1}$, vs. Ag/AgCl; A) cyclic voltammogram; B) plot $\Delta m$ vs $Q$ for anodic process; grey parts of the curve - trend lines for the $\Delta m = f(Q)$ relationship.

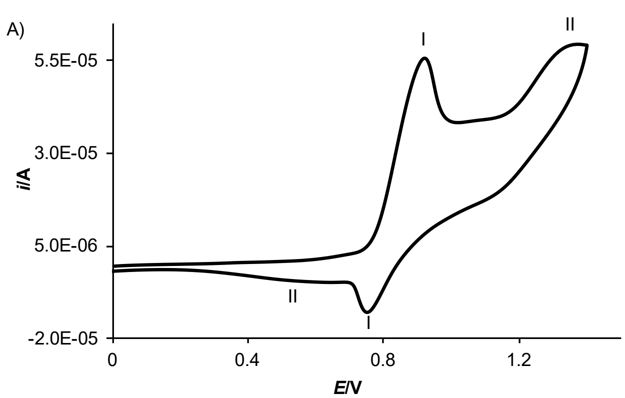

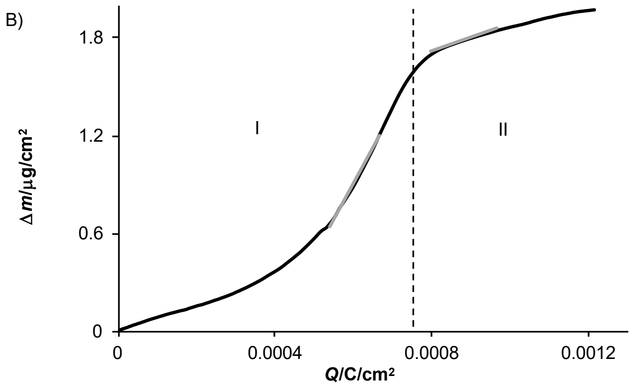


**Figure S7**. *Poly*[Ni(salcn(Bu))] (1 electropolymerization cycle) in $TBABF_4/CH_2Cl_2$, Pt/quarzglas , $v = 0.05\ V{\cdot}s^{-1}$, vs. Ag/AgCl; A) cyclic voltammogram; B) plot Δ*m* vs *Q* for anodic process; grey parts of the curve - trend lines for the Δ*m* = f(*Q)* relationship.

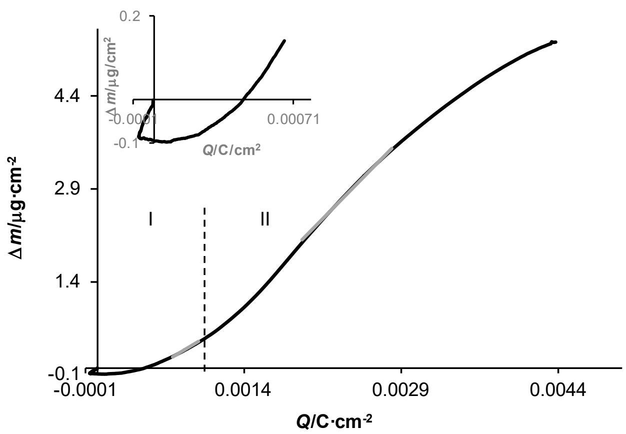


**Figure S8**. Plots Δ*m* vs *Q* for *poly*[Ni(salcn)] for anodic process (1 electropolymerization cycle) in $TBAPF_6/CH_2Cl_2$, Pt/quarzglas , $v = 0.01\ V{\cdot}s^{-1}$, vs. Ag/AgCl; grey parts of the curve - trend lines for the Δ*m* = f(*Q)* relationship.

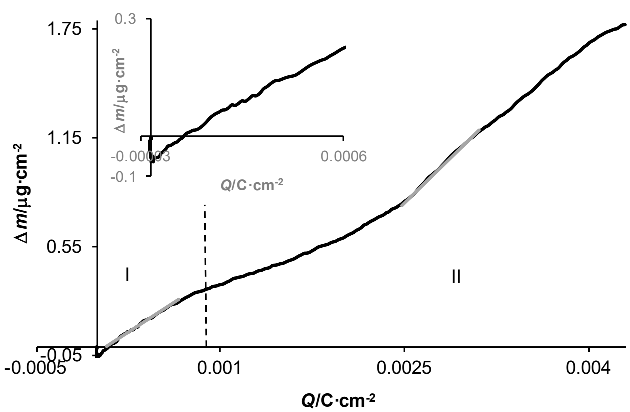


**Figure S9**. Plots Δ*m* vs *Q* for *poly*[Ni(salcn)] for anodic process (1 electropolymerization cycle) in $TBABF_4/CH_2Cl_2$, Pt/quarzglas , $v = 0.01\ V{\cdot}s^{-1}$, vs. Ag/AgCl; grey parts of the curve - trend lines for the Δ*m* = f(*Q)* relationship.

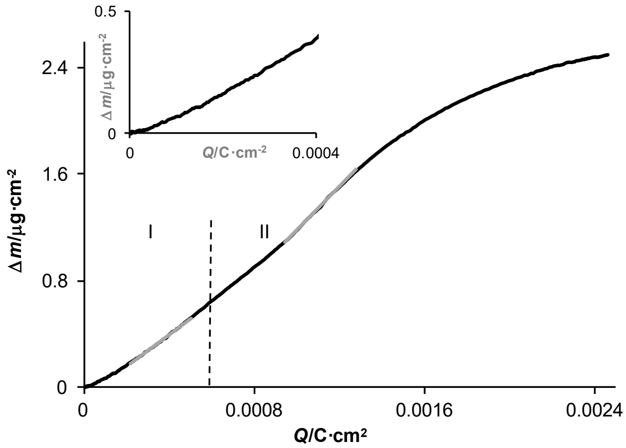


**Figure S10**. Plots $\Delta m$ vs $Q$ for *poly*[Ni(salcn)] for anodic process (1 electropolymerization cycle) in $TBAPF_6/CH_2Cl_2$, Pt/quarzglas , $v = 0.05$ V·s$^{-1}$, after reduction 40 s at 0 V, vs. Ag/AgCl; grey parts of the curve - trend lines for the $\Delta m = f(Q)$ relationship.

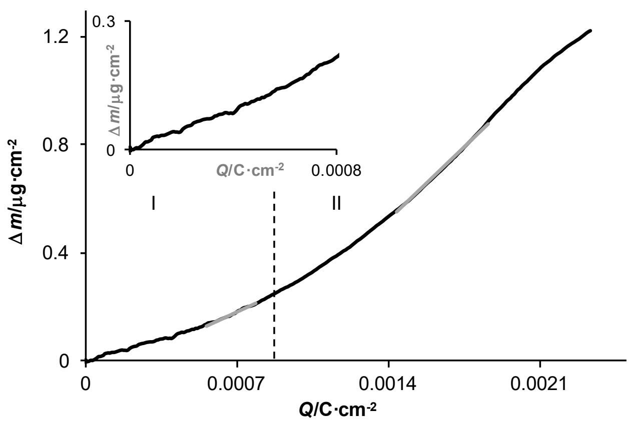


**Figure S11**. Plots $\Delta m$ vs $Q$ for *poly*[Ni(salcn)] for anodic process (1 electropolymerization cycle) in $TBABF_4/CH_2Cl_2$, Pt/quarzglas , $v = 0.05$ V·s$^{-1}$, after reduction 40 s at 0 V, vs. Ag/AgCl; grey parts of the curve - trend lines for the $\Delta m = f(Q)$ relationship.

A)

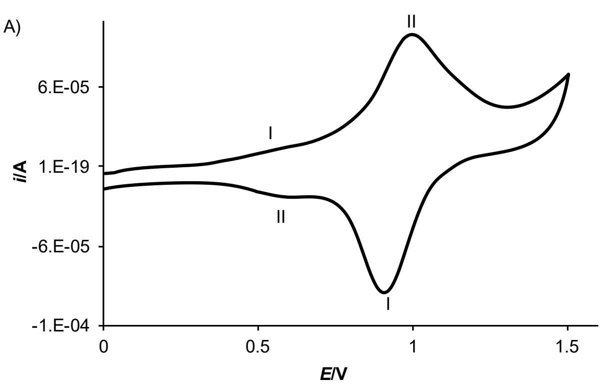

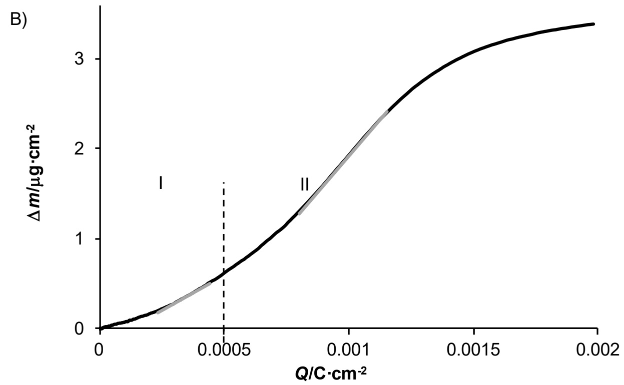


**Figure S12**. Figure S12. *Poly*[Ni(salcn)] (1 electropolymerization cycle) in $TBAPF_6$/MeCN, Pt/quarzglas , $v = 0.05$ V·s$^{-1}$, vs. Ag/AgCl; A) cyclic voltammogram; B) plot $\Delta m$ vs $Q$ for anodic process; grey parts of the curve - trend lines for the $\Delta m$ = f($Q$) relationship.

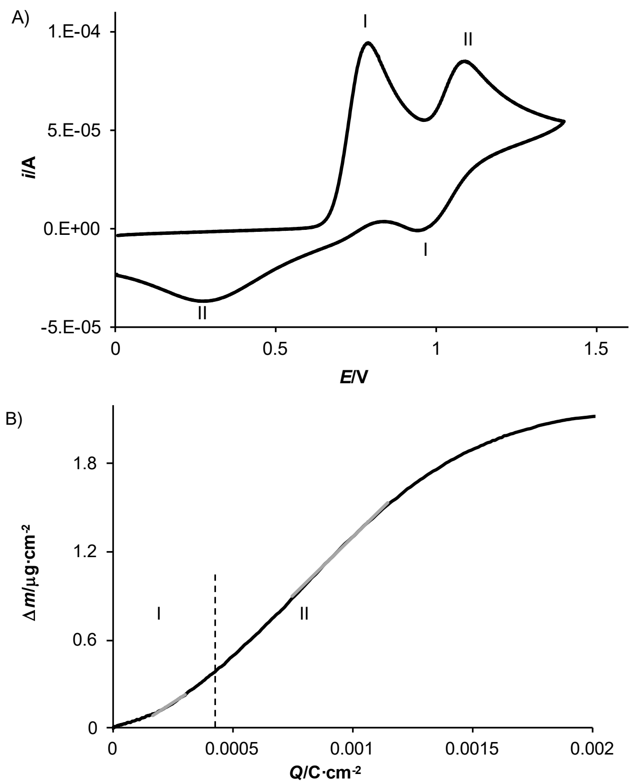


**Figure S13**. *Poly*[Ni(salcn)] (1 electropolymerization cycle) in $TBABF_4$/MeCN, Pt/quarzglas , $v = 0.05$ V·s$^{-1}$, vs. Ag/AgCl; A) cyclic voltammogram; B) plot $\Delta m$ vs $Q$ for anodic process; grey parts of the curve - trend lines for the $\Delta m$ = f($Q$) relationship.

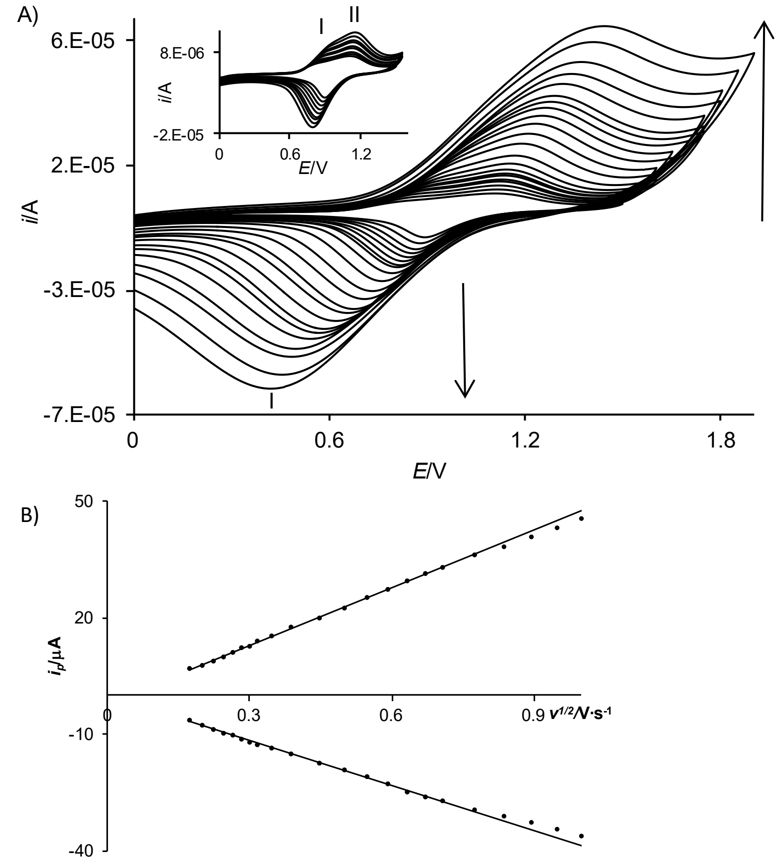


**Figure S14**. *Poly*[Ni(salcn)] (10 electropolymerization cycles) in $TBAClO_4/CH_2Cl_2$, Pt, $v = 0.03$ - 1 $V{\cdot}s^{-1}$, vs. Ag/AgCl; A) the lower part - cyclic voltammograms; the upper part – voltammograms for $v = 0.01 – 0.09$ $V{\cdot}s^{-1}$; B) plots $i_p$ vs $v^{1/2}$ for oxidation and reduction processes.

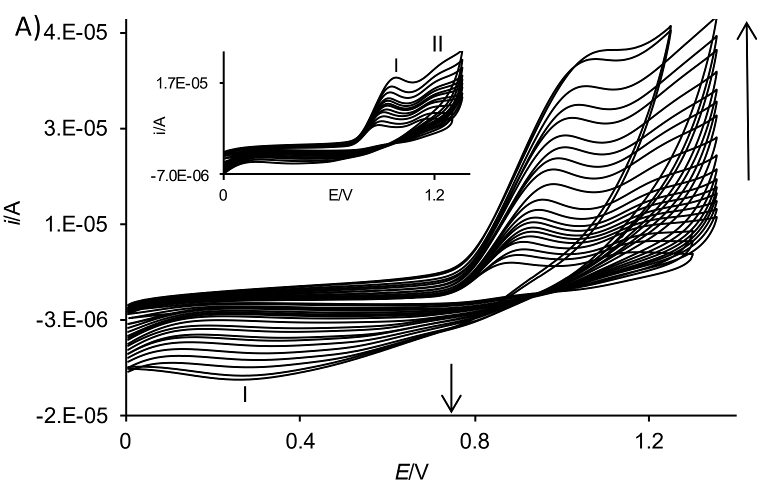

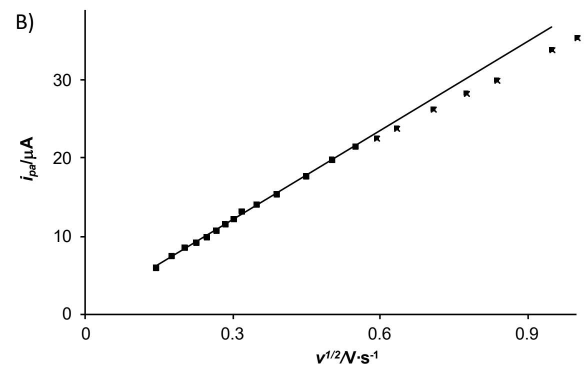


**Figure S15**. *Poly*[Ni(salcn)] (3 electropolymerization cycles) in $TBABF_4/CH_2Cl_2$, Pt, $v = 0.02$ - 1 V·s$^{-1}$, vs. Ag/AgCl; A) the lower part - cyclic voltammograms; the upper part – voltammograms for $v = 0.01 – 0.15$ V·s$^{-1}$; B) plot $i_{pa}$ vs $v^{1/2}$ for oxidation process.

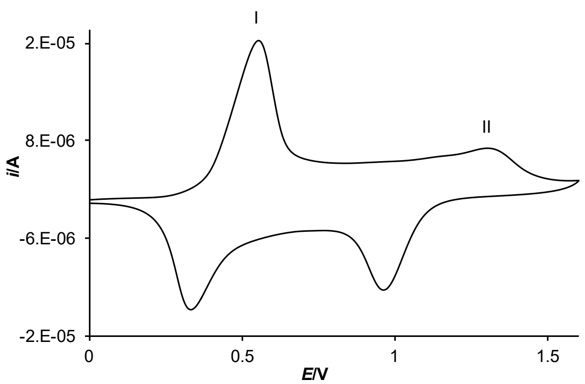


**Figure S16**. Cyclic voltammogram of *poly*[Ni(salcn(Me))] (10 electropolymerization cycles) in $TBAClO_4/CH_2Cl_2$, Pt, $v = 0.05$ V·s$^{-1}$, vs. Ag/AgCl.

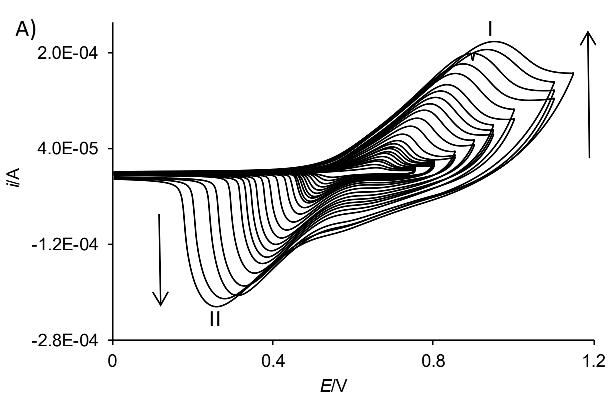

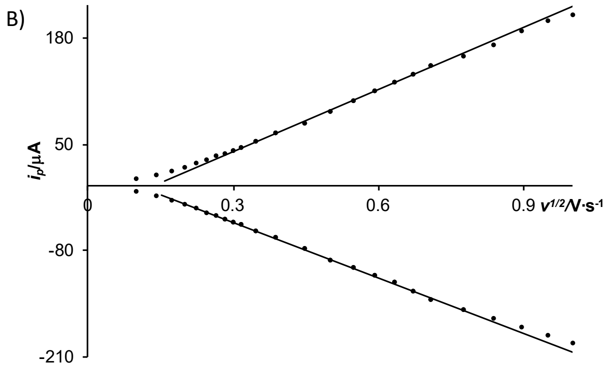


**Figure S17**. *Poly*[Ni(salcn(Me))] (15 electropolymerization cycles) in $TBABF_4/CH_2Cl_2$, Pt, $v = 0.01 - 1$ V·s$^{-1}$, vs. Ag/AgCl; A) cyclic voltammograms for one-step process, peak notations were used adequate to peak designation in a two-step process, see Figure 3; B) plots $i_{pa}$ vs $v^{1/2}$ for oxidation and reduction processes.

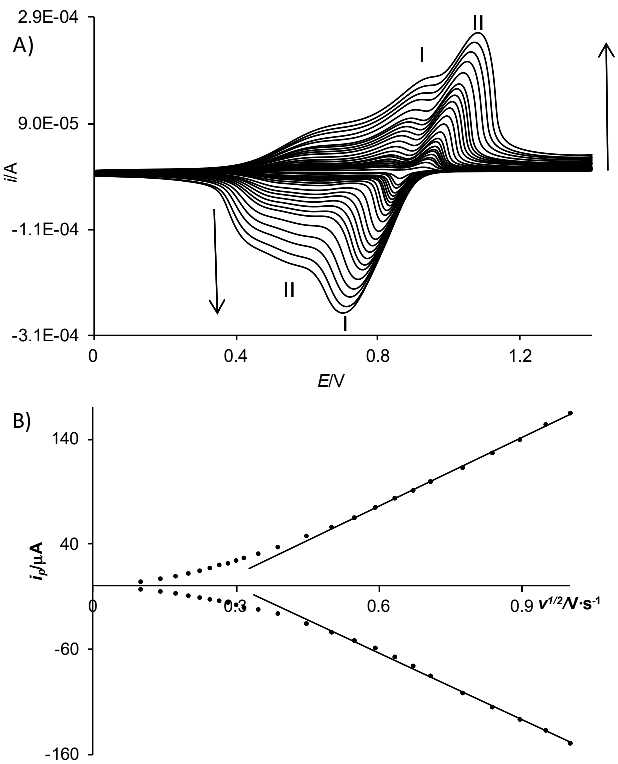

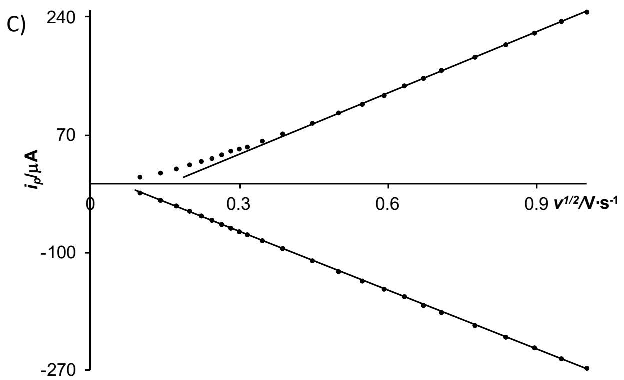


**Figure S18**. *Poly*[Ni(salcn(Bu))] (25 electropolymerization cycles) in $TBAClO_4/CH_2Cl_2$, Pt, $v = 0.01 - 1$ V·s$^{-1}$, vs. Ag/AgCl; A) cyclic voltammograms; B) plots $i_p$ vs $v^{1/2}$ for I$^{st}$ oxidation step of the process and II$^{nd}$ reduction step*;* C) plots $i_p$ vs $v^{1/2}$ for II$^{nd}$ oxidation step of the process and I$^{st}$ reduction step.

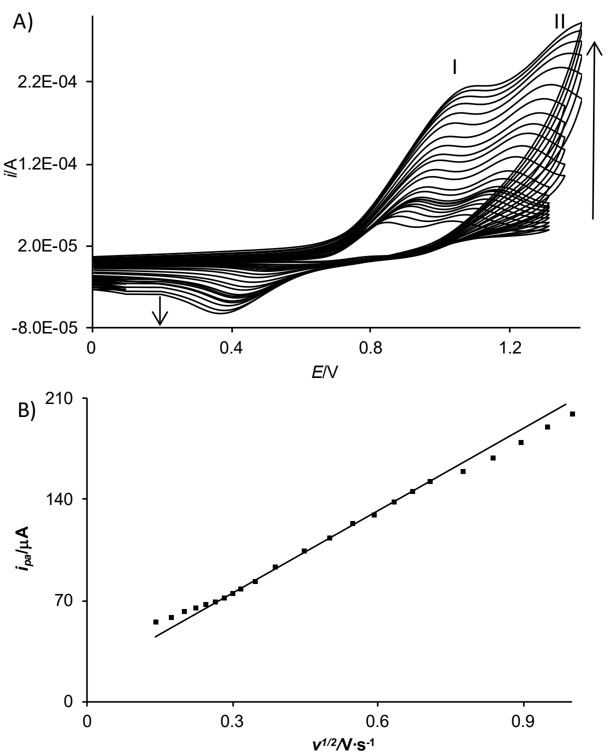

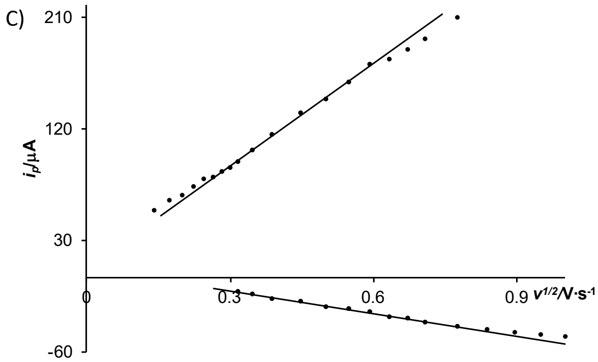


**Figure S19**. *Poly*[Ni(salcn(Bu))] (25 electropolymerization cycles) in $TBABF_4/CH_2Cl_2$, Pt, $v = 0.02$ - 1 V·s$^{-1}$, vs. Ag/AgCl; A) cyclic voltammograms; B) plot $i_p$ vs $v^{1/2}$ for I$^{st}$ oxidation step of the process*;* C) plots $i_p$ vs $v^{1/2}$ for II$^{nd}$ oxidation step of the process and I$^{st}$ reduction step.

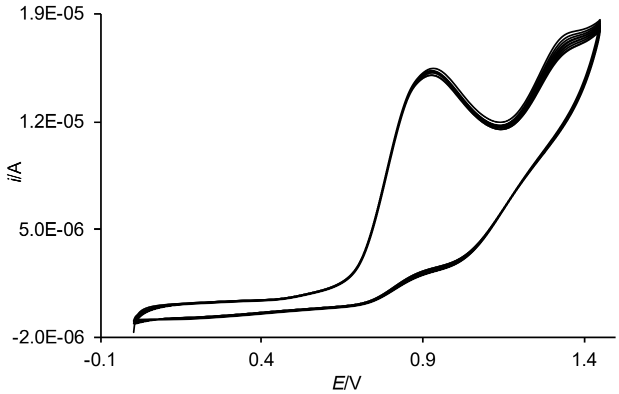


**Figure S20**. Cyclic voltammograms *of poly*[Ni(salcn)], 1$^{st}$-10$^{th}$ cycle, in $TBABF_4/CH_2Cl_2$, Pt, $v = 0.05$ V·s$^{-1}$, vs. Ag/AgCl; after 5 electropolymerization cycles.

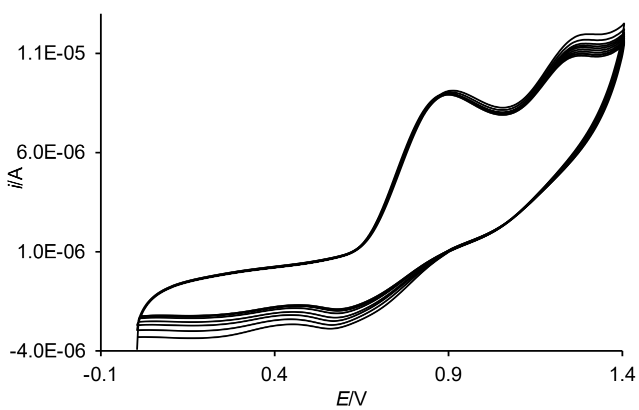


**Figure S21**. Cyclic voltammograms *of poly*[Ni(salcn(Bu))], 1$^{st}$-10$^{th}$ cycle, in $TBABF_4/CH_2Cl_2$, Pt, $v = 0.05$ V·s$^{-1}$, vs. Ag/AgCl; after 5 electropolymerization cycles.

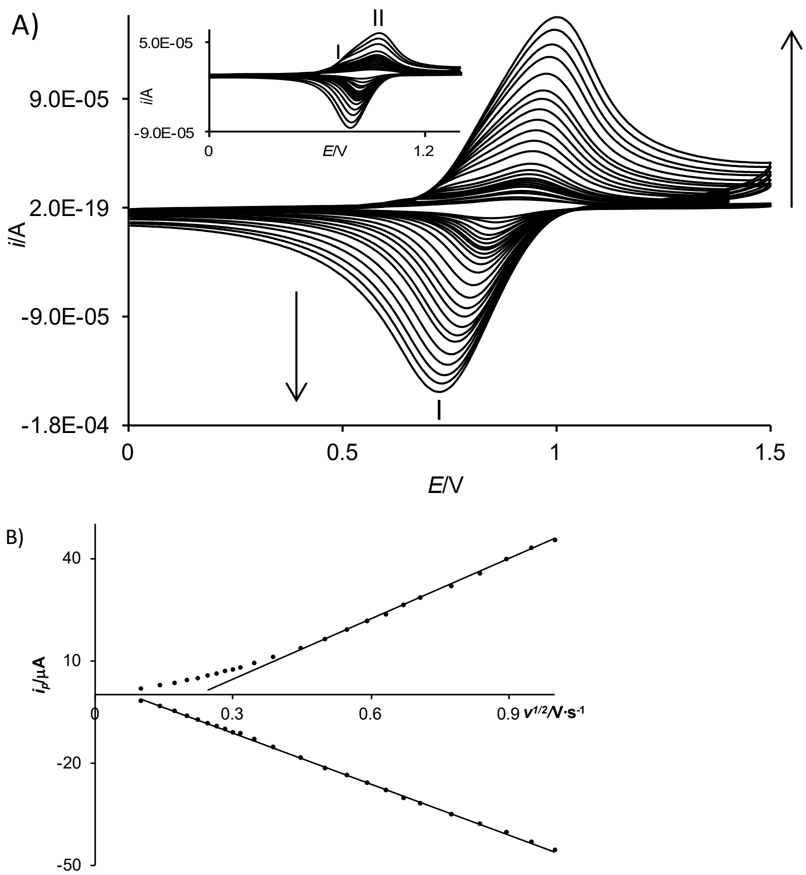


**Figure S22**. *Poly*[Ni(salcn)] (3 electropolymerization cycles) in TBAClO$_4$/MeCN, Pt, $v$ = 0.01 - 1 V·s$^{-1}$, vs. Ag/AgCl; A) the lower part - cyclic voltammograms, the upper part – voltammograms for $v$ = 0.01 – 0.25 V·s$^{-1}$; B) plots $i_{pa}$ vs $v^{1/2}$ for oxidation and reduction processes.

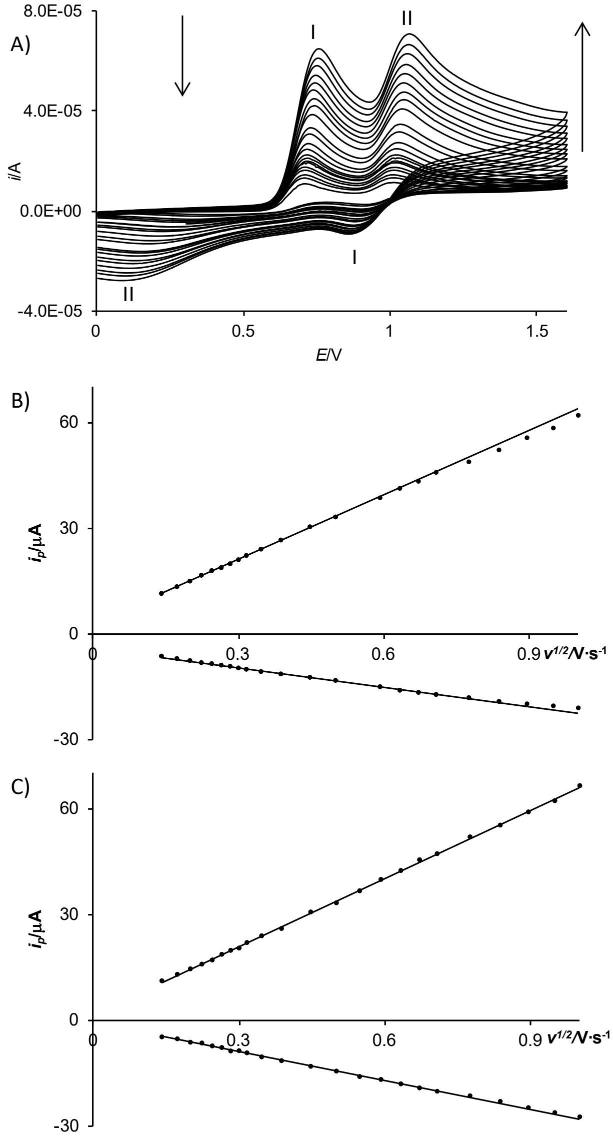


**Figure S23**. *Poly*[Ni(salcn)] (3 electropolymerization cycles) in $TBABF_4$/MeCN, Pt, $v = 0.02 - 1$ V·s$^{-1}$, vs. Ag/AgCl; A) cyclic voltammograms; B) plots $i_p$ vs $v^{1/2}$ for I$^{st}$ oxidation step of the process and II$^{nd}$ reduction step*;* C) plots $i_p$ vs $v^{1/2}$ for II$^{nd}$ oxidation step of the process and I$^{st}$ reduction step.